Daylight photoluminescence imaging of photovoltaic systems using inverter-based switching

t trupke[1], Juergen W. Weber[1], Oliver Kunz[1], C. Knaack[2], D. Chung[2], A. Barson[3], A. Slade[1], Z. Ouyang[1], and H. Gottlieb[1]

[1]University of New South Wales School of Photovoltaic and Renewable Energy Engineering
[2]SMA Solar Technology AG
[3]Gentari / Wirsol

April 22, 2024

Abstract

Daylight photoluminescence imaging of crystalline silicon photovoltaic modules is demonstrated for modules embedded in rooftop and utility-scale systems, using inverters to electrically switch the operating point of the array. The method enables rapid and high-quality luminescence image acquisition during the day, unlocking efficient performance and quality monitoring without the need to connect specific electrical hardware or to make any modifications to the system wiring. The principle of the measurement approach is discussed and experimental results from a 10 kW $_{DC}$ residential rooftop system and from a 149 MW $_{DC}$ utility-scale photovoltaic power plant are presented. Measurements were performed using commercial inverters without modifications to the inverter hardware or firmware. In the case of the utility-scale power plant, the daylight photoluminescence image acquisition of modules connected to a central inverter was obtained from a remote piloted aircraft. Data analysis includes the conversion of photoluminescence image data into implied voltage differences.

Daylight photoluminescence imaging of photovoltaic systems using inverter-based switching

J.W. Weber, O. Kunz, C. Knaack[1], D. Chung[1], A. Barson[2]

A. Slade, Z. Ouyang, H. Gottlieb, T. Trupke*

The University of New South Wales, Sydney, Australia

[1] SMA Australia

[2] Gentari / Wirsol Australia

*E-mail address: t.trupke@unsw.edu.au

Abstract

Daylight photoluminescence imaging of crystalline silicon photovoltaic modules is demonstrated for modules embedded in rooftop and utility-scale systems, using inverters to electrically switch the operating point of the array. The method enables rapid and high-quality luminescence image acquisition during the day, unlocking efficient performance and quality monitoring without the need to connect specific electrical hardware or to make any modifications to the system wiring. The principle of the measurement approach is discussed and experimental results from a 10 kW_{DC} residential rooftop system and from a 149 MW_{DC} utility-scale photovoltaic power plant are presented. Measurements were performed using commercial inverters without

modifications to the inverter hardware or firmware. In the case of the utility-scale power plant, the daylight photoluminescence image acquisition of modules connected to a central inverter was obtained from a remote piloted aircraft. Data analysis includes the conversion of photoluminescence image data into implied voltage differences.

Keywords: Photoluminescence imaging, crystalline silicon, photovoltaics, solar modules

Background and Motivation

There is a growing consensus that the exponential growth of the cumulatively installed photovoltaic (PV) capacity will continue unabated over coming decades. A large group of experts have forecast that sustained 25% compounding annual growth will result in 70-80 TW_{DC} of installed PV capacity by 2050, to be supported by 3-4 TW_{DC} of annual module manufacturing and module installations . The global annual electricity consumption in 2022 was estimated by the International Energy Agency (IEA) to be 28,777 TWh. For comparison, in the above scenario the electricity generated from PV alone will reach an estimated 130,000 TWh per annum, thus exceeding today's total worldwide annual electricity generation and consumption by more than four times. Consequently, PV will rapidly become the main source of global primary energy over coming decades.

PV modules based on single-junction crystalline silicon solar cells dominate industrial manufacturing and commercial PV deployment today and will remain the dominant technology for the foreseeable future, possibly over coming decades . Power production yield from PV power plants can be affected by module quality and integrity in multiple ways. These include manufacturing issues, damage occurring during transport and installation, degradation during operation under harsh environmental conditions and catastrophic weather events such as hailstorms, among others. With industrial silicon modules now rapidly approaching their theoretical efficiency limit, longevity and module quality are more important than ever since re-powering of solar systems and early retirement of PV modules are no longer economically viable options . For these reasons, systematic in-field testing and monitoring are of increasing importance.

Electroluminescence (EL) and photoluminescence (PL) imaging emerged around 2005 as powerful diagnostic tools for device and process optimisation, process monitoring and quality testing. PL imaging is now used routinely for PV research and development purposes, whereas EL imaging has become an integral part of quality testing in high-volume cell- and module manufacturing. A wealth of information about material and device defects is contained in luminescence image data, making this measurement principle an ideal candidate for field inspection of modules in operating solar systems. Moreover, since specific information about the presence of defects or degradation that is contained in luminescence image data cannot be gleaned in any other fashion, we are of the firm view that luminescence imaging must become an integral, potentially dominant part of routine field testing, complemented by other inspection methods such as thermal imaging , visual inspection and performance data analysis .

Monochromatic or narrow-band light sources such as lasers or light emitting diodes are commonly employed for laboratory PL imaging applications. Alternatively, and only for outdoor applications during daytime, the sun itself can be used as the excitation source in so-called daylight PL imaging (DPL) applications. A significant technical challenge for DPL imaging, however, is the separation of the luminescence signal emitted by crystalline silicon solar cells from the (typically orders of magnitude more intense) reflected sun light.

An elegant technical solution to this problem is based on PL image acquisition within an ultra-narrow atmospheric spectral absorption band in which incident sunlight is almost completely blocked by water vapor absorption and which coincides spectrally with the room temperature emission from crystalline silicon . Other solutions are based on a lock-in type approach, whereby the emitted luminescence is modulated by manipulating the electrical operating point of modules, for example between open circuit (OC) and the maximum power point (MPP). The PL image is obtained as the difference between two (or more) images, which is the approach we also take in this study.

Different methods to achieve the required variation of a module's electrical operating point have been demonstrated, including the electrical connection of specialised switching electronics to the module terminals, non-contact module-level optical modulation and non-contact string-level optical modulation. A topical review of these methods was presented in .

Using the PV inverter as a means of rapidly switching between different operating points offers an additional solution. Vukovic et al. demonstrated DPL image acquisition during IV curve sweeps, which some residential inverters commonly perform in certain intervals to determine the global MPP . However, the operating point of a PV string or array can also be deliberately changed via the PV inverter, which allows the acquisition of daylight PL images in a more controlled way . Preliminary results from a demonstration of controlled variation of the operating point, achieved with a customised inverter, and performed on a small test set-up, were recently presented by Koester et al. .

Here, we demonstrate DPL image acquisition using controlled inverter switching on operational PV systems and on a much larger scale, whereby the operating points of all modules connected to an individual inverter are actively manipulated. The method is demonstrated (i) on a 12 KW_{DC} rooftop system located in Sydney, and (ii) on a 2.75 MW_{DC} central inverter in a 149 MW_{DC}Australian utility-scale solar farm. Both sets of experiments were conducted using SMA inverters, without modifications to the hardware or firmware. Actively controlling the inverter requires knowledge about specific inverter settings and capabilities. Modulation settings and associated safe operation limits as well as details of the required communication protocols and access permissions were discussed with the inverter manufacturer (SMA) prior to all experiments presented here. This is a requirement for future experiments of this nature. Photoluminescence image acquisition in the utility-scale solar farm was achieved from a remote piloted aircraft (RPA), which we consider to be the most practical and economical solution for rapid DPL inspection of solar assets.

Experimental

Rooftop system

The inverter-based switching method for DPL image acquisition was demonstrated first on a 12 kW_{DC} / 10 kW_{AC} residential rooftop system at Wylie's Baths in the eastern suburbs of Sydney. The PV system was commissioned in March 2021 and consists of 35 bifacial 350 W_p glass-glass modules, each containing 120 half-cell PERC cells with a nominal open circuit voltage of 682 mV per cell. The modules are arranged in two series-connected strings that are connected to the DC inputs of a 10 kW SMA Sunny-boy Tripower inverter. DPL measurements were performed on a sunny day in April 2023 using an Indium Gallium Arsenide (InGaAs) camera with a resolution of 1280 x 1024 pixels in conjunction with near-infrared camera objectives with focal lengths ranging from 12.5 mm to 50 mm. A 25 nm bandpass filter with a centre wavelength of 1,137 nm was mounted in front of the camera lens for all measurements to exploit a broad atmospheric absorption band that coincides with the emission spectrum from crystalline silicon at room temperature. The filter increases the relative proportion of the PL signal in each individual image, as previously demonstrated and as discussed in more detail elsewhere .

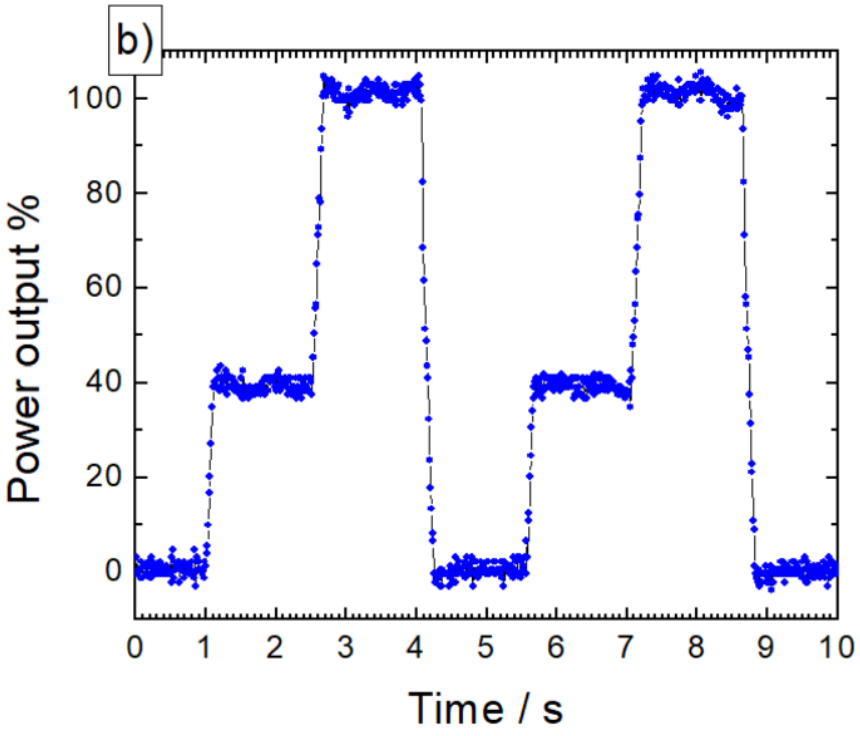

The camera was mounted on a remote-controlled motorised pan and tilt head that was attached to an aluminium pole serving as an improvised camera mount. The pole caused significant camera shaking in the windy conditions present during testing. An ethernet connection was used for communication with the inverter to enable periodic switching of the operating point of all modules in this PV system and setting of the operating point to any value between MPP and OC conditions.

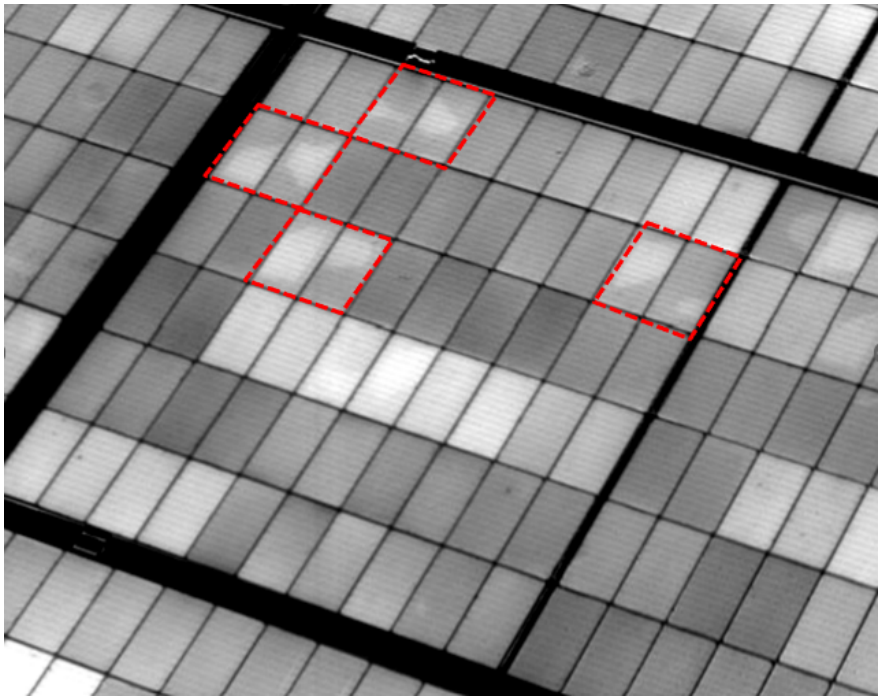

A current clamp connected to a digital oscilloscope was used to monitor the temporal variation of the electrical current into the DC inverter inputs. Fig. 1 shows the normalised DC current flowing into one of the inverter inputs during two different switching regimes, reflecting relative power output from the system. In Fig.1(a) the current trace reflects a two-step switching process, whereby the operating point of the system is switched between MPP, at which 100% of the available power is extracted and OC, at which the DC current into the inverter and the extracted power are zero. Note that under OC condition the cells embedded in the modules emit maximum luminescence intensity, whereas at MPP about 95% of the photogenerated carriers are extracted, reducing the luminescence intensity to close to zero. In Fig.1(b) the operating point is periodically switched in three distinct steps, including an interim step at which 40% of the MPP current (I_{mpp}) is extracted from the module, resulting in approximately 40% of the maximum power being extracted. While not the focus of this paper, the ability to switch between different operating points enables calculation of image differences that allow differentiating series resistance variations from recombination defects, as demonstrated in the context of daylight PL imaging by Bhoopathy et al. .

The switching of the power output from 100% to zero takes place in < 150 ms, but due to a long dwell time of about 1.5 s the overall cycle time is about 3 s. This comparatively long cycle time was chosen intentionally in our proof-of-concept studies reported here as a conservative setting. We anticipate being able to perform switching at considerably higher frequencies and with shorter switching times in the near future, noting though that for residential rooftop applications, as discussed here, the above switching rate is sufficient to enable rapid high resolution DPL inspection of all modules of a system within a few minutes.

Individual camera images were acquired with exposure times between 15 ms and 20 ms. Image registration was applied to improve DPL image quality, minimizing DPL image imperfections caused by very significant camera shake. It is noted that camera shake does not notably affect the quality of individual camera images, given the above short exposure times. However, it results in lateral offsets between images, producing artefacts when difference images are calculated. Image registration prior to image subtraction eliminates this unwanted effect.

Fig.2 shows two PL images acquired using inverter-based switching on the residential rooftop system at Wylie's Baths, as described above. From the fixed camera position the 50mm focal length lens that was used

for these measurements provides close-up DPL images showing half a module to one full module, depending on the specific module location on the roof (i.e. distance to the camera). Each DPL image was calculated from 10 image pairs.

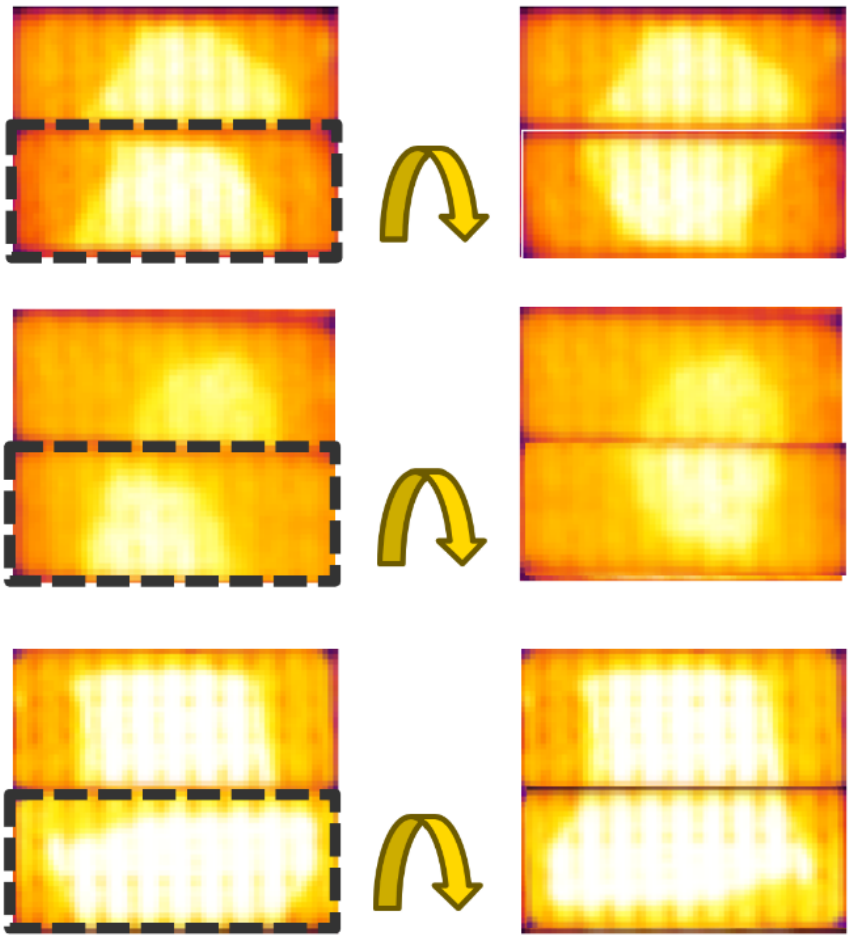

The DPL image shown in Fig. 2(a) shows a module half with 60 half-cells, exhibiting significant PL intensity variations between half cells, indicative of voltage variations and a strong indication of module degradation. The image also clearly shows a several centimetre-long microcrack (red circle), various point-like defects and the front bus bars, demonstrating the excellent image quality that was achieved with inverter-based DPL imaging.

Fig.2(b) shows a section of another module from the same rooftop system, containing various examples of a defect that we have named the *Yin Yang* defect, and which we first reported recently . These defects appear in pairs of half-cells, whereby the patterns match when one half cell is de-rotated computationally. Tens of examples of this defect were observed across different modules within the Wylie's Baths rooftop system.

We observed the same defect during earlier field work, using the optical string modulation technique in an Australian utility-scale solar farm, where tens of thousands of glass-glass half-cell PERC modules exhibited this defect after only approximately 1.5 years of operation in the field. Importantly, the modules in that solar farm were from a different brand compared to the residential system discussed above. Fig.3 shows a DPL image from that earlier study of a module that exhibits several examples of the Yin Yang defect. The assembly of half-cell modules in mass production involves breaking a full cell into halves and rotating one

half-cell by 180 degrees prior to layup in the module. As shown in Fig.3 (three examples are highlighted in the original image with white squares), the computational de-rotation of one half-cell in each pair results in perfect matching of the defect patterns, demonstrating that the defect was already present in the full cell. DPL images of non-fielded modules of the same module series did not show these defects, the presence of the defects is thus a strong sign of module degradation due to field exposure. We conclude that this defect is present in the full cell as a latent defect that only becomes activated by field exposure. Interestingly, we find that the luminescence intensity from the higher-intensity regions within these defects is comparable to that of modules from the same series that have not been exposed to sunlight and which do not show these defects. This suggests that the bright regions have degraded less strongly due to field exposure, compared to the surrounding dark regions and that prevention or mitigation of these defects could result in significant improvements in system power output. The nature of the underlying degradation mechanism is currently unclear and subject to ongoing investigations, which are not the focus of this publication.

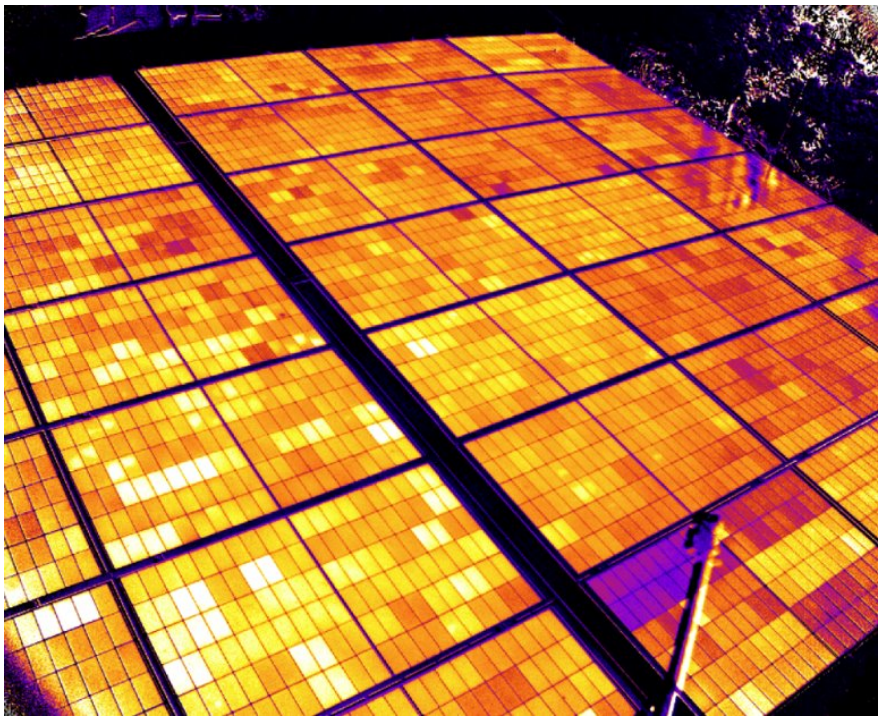

A significant practical benefit of inverter-based modulation is the ability to take DPL images of all modules that are connected to the same inverter, either sequentially and with high spatial resolution (close-up imaging), as shown in Fig.2, or simultaneously in a single overview image, with reduced spatial resolution. The larger field of view required for an overview image can be achieved either by moving the camera further away from the target or by using a camera objective lens with a shorter focal length. Fig.4 shows a DPL image of the rooftop system that was acquired with a 12.5mm focal length lens. The acquisition of the full roof in a single DPL image could not be achieved in this study, simply due to limitations with respect to the positioning of the camera using our improvised camera mount (i.e. the camera could not be moved further away). The image contains a few artefacts, including the effect of optical reflections of surrounding trees that were moving in the wind (green arrow in Fig.4). Note that reflections of stationary objects do not cause such artefacts, since they cancel out in the image difference calculation. We also observe an artefact associated with the shadow cast by the (shaking) mounting pole and the camera (blue arrow). The latter effect causes the top third of one module to appear darker. The shading effects by the camera can be avoided by more careful placement of the camera, in particular, when images are acquired using an RPA (as demonstrated in the following section). Artefacts associated with objects such as plants, buildings or other architectural

features are generally not a concern for large utility-scale systems and may be avoidable in applications on residential PV systems with careful planning and timing of experiments.

Utility-scale System

Utility-scale inverter-based DPL imaging was demonstrated at a 149 MW_{DC} solar farm in Australia in October 2023. The farm became fully operational in March 2021, utilising 400 W monofacial half-cell modules on single-axis trackers. The modules feature PERC solar cells with a nominal open-circuit voltage of 690mV per cell according to the module specifications. The farm uses 2.75 MW SMA central inverters (Sunny Central 2750-EV), with approximately 9,000 modules connected to each inverter. For the proof of concept of large-scale DPL image acquisition using inverter-based modulation reported here, only one 2.75 MW inverter was switched. As a precaution, only <60% of the inverter's rated DC power was switched at any time (e.g. between 90% and 30% of maximum power) to avoid potential risks of thermal cycling on the power electronics. DPL image acquisition was achieved using the same InGaAs camera (1280 x 1024 pixel resolution) that was used for the data acquired on the rooftop section discussed above. The camera was mounted on a customised DJI M600 hexacopter RPA, the latter running custom image acquisition software on an on-board computer. A Gremsy gimbal was used to stabilise the camera, enabling image acquisition with up to 50 ms exposure time for the individual image without significant loss of image sharpness due to camera shake. Images were acquired using a 50 mm focal length objective lens equipped with the same bandpass filter described above.

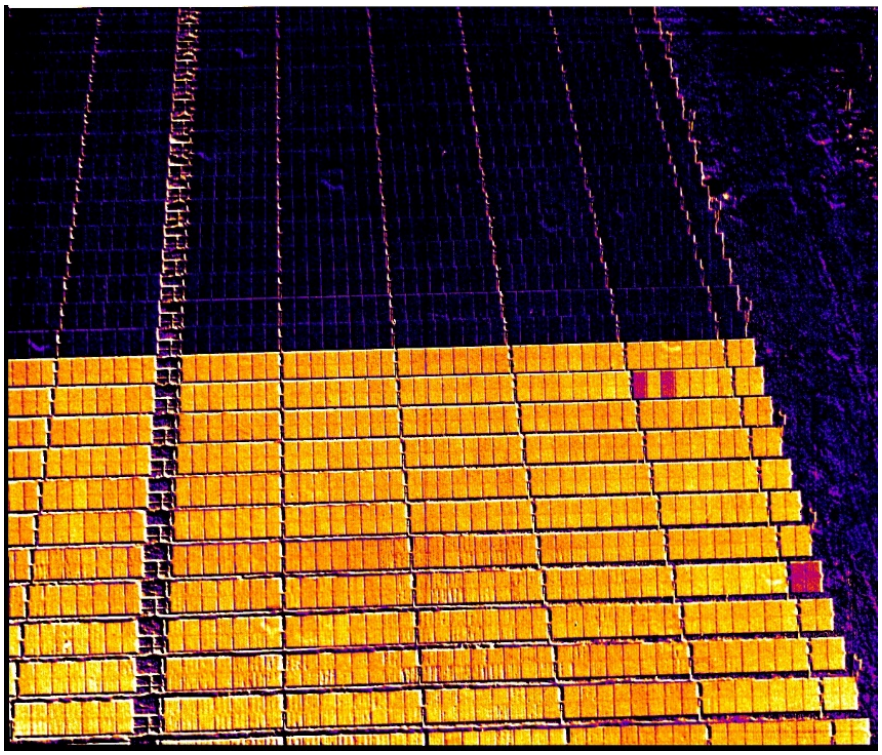

Fig.5 shows a DPL image of a large section of the solar farm, containing approximately 1,200 PV modules in one single image. Only modules located in the bottom half of this image are connected to the inverter that was switched, i.e. only half of the modules yield a PL image, the other half appearing dark in the difference image, as expected. Further, the image includes a grassy area to the right of the PV array, which also appears dark. The image was calculated from 20 individual near-infrared camera images. We observe

an average PL signal count in the section containing the switched modules of 290 counts, whereas the count rate in both the grassy area and the non-switched section is below 10 counts. Four modules in the image stand out in red. They exhibit considerably lower PL counts compared to all other modules in that section of the solar farm. The PL intensity from these modules is approximately 53% compared to the surrounding modules.

Quantitative analysis of luminescence intensities from solar cells is based on the Generalised Planck Equation , predicting an exponential relationship between the emitted luminescence intensity and the diode voltage of the device. In simplified form that relationship can be written as

$$I_{\mathrm{PL}} = Ce^{\left(\frac{\mathrm{qV}}{\mathrm{kT}}\right)} \quad (1)$$

where I_{PL} is the emitted luminescence intensity,k is Boltzmann's constant, q is the elementary charge,T is the sample temperature and V is the diode voltage. The so-called thermal voltage kT/q has a value of about 25.85 mV at room temperature. The calibration constant C in Eq.1 depends on various sample specific geometric and optical sample parameters, on the spectral sensitivity of the detection system and on various measurement parameters. The accuracy of obtaining implied voltages from luminescence signals is therefore linked to the ability to accurately determine the constant C . By contrast, it follows from Eq.1 that the ratio of two luminescence signals, $I_{PL,1}$ and$I_{PL,2}$ respectively, can be converted into a voltage difference $\Delta^{\sim}$via

$$V = \frac{\mathrm{kT}}{q} \ln \frac{I_{PL,1}}{I_{PL,2}}. \quad (2)$$

provided that the calibration constant C can be assumed to be the same for the two luminescence measurements. That is the case if measurements are conducted with the same measurement system (as is the case here) and with identical measurement parameters (as is also the case here) and either on the same sample at different times or under different bias conditions or on different samples which can be assumed to have similar optical properties.

Eq. 2 predicts 16.5 mV lower voltage per cell for the four modules that appear in Fig.5 with 53% lower PL counts. During our experiments we noted some variation in optical properties between modules in this solar farm in the near infrared spectral range that is defined by the bandpass filter mounted on the camera lens. A detailed quantitative analysis of DPL results obtained from this solar farm, including the expected minor impact of these optical variations is currently underway and will be reported elsewhere, noting however that the focus of this publication is the demonstration of the inverter-based DPL image acquisition principle. We would like to emphasise, that the quantitative analysis of DPL image variations between cells or modules of the same type in terms of voltage variations according to Eq.2 is well established. For validation purposes we performed separate experiments on modules at a UNSW outdoor test system. These measurements confirmed that the accuracy of implied voltage differences between modules from PL images is on the order of +/- 2 mV per cell when PL image data is compared to measured terminal voltages under well controlled experimental conditions.

The DPL image example in Fig.5 demonstrates, for the first time, the ability to simultaneously acquire PL images of very large numbers of PV modules, in similar fashion to what is currently common practice with RPA-based thermal infrared imaging. RPA-based camera deployment enables not only the acquisition of images of large sections of the farm from a high vantage point, but also convenient and rapid change of the camera field of view by variation of the distance to the target. For the experiments discussed above positioning of the RPA prior to image acquisition was achieved with manual RPA flight control. For the near future we envisage automated mapping of solar farms with pre-programmed flight paths and way points, as is current practice for thermal inspection. In this scenario we envisage the use of high-level overview PL imaging data captured from RPAs, as shown in Fig.5, in combination with either close-up RPA-based imaging or high-fidelity imaging from the ground. This will enable rapid overview images to be acquired first, followed by more detailed inspection of specific modules or farm sections with suspected defects.

Discussion

The ability to acquire outdoor DPL images of entire PV systems or of large sections of solar farms using inverter-based modulation is a very significant step towards cost effective and commercially viable daylight luminescence imaging of large utility scale solar systems. The analysis of relative PL intensities is a particularly powerful quantitative tool to assess voltage variations between and within modules, and to quantify module degradation. Of particular importance in this context is the robustness of PL image data against variations in sample temperature. Zafirovska et al. showed that the temperature coefficient of implied voltages that are derived from luminescence is about ten times lower than the temperature coefficient of the terminal voltage. This is particularly relevant here since measuring temperatures on PV modules in the field with good accuracy is generally difficult to achieve. While such accurate temperature measurements are a key requirement for the analysis of terminal voltage measurements of fielded modules, it is not required for quantitative PL image analysis due to the low temperature sensitivity of the PL signal.

The inverter-based manipulation of the operating point of large numbers of modules that are connected to specific inverters in combination with RPA-based image acquisition is an elegant solution to inspect large solar assets, and to find faulty modules or determine module degradation. No modifications to the system wiring are required, it can be performed during the day and does not require large and heavy equipment such as power supplies and generators to be brought on site. Daylight PL imaging also avoids additional hazards (electrical, night-work) and administrative difficulties associated with working at nighttime.

Summary and Conclusions

High quality daylight photoluminescence image acquisition of crystalline silicon solar modules in both rooftop and utility-scale solar farms using electrical modulation of the operating point of modules connected to an inverter was demonstrated. Measurements were performed by manipulating the operating point of modules using existing functionality of commercial inverters, without specific customisation of either hardware or firmware, without any modifications to the PV system's electrical wiring and without utilising additional large power electronic equipment, such as generators and power supplies. Importantly, measurements were performed in daylight during regular working hours, avoiding the administrative and practical complications and risks associated with nighttime operation.

It was shown that close-up high-resolution and high-quality images of individual modules enable the detection of microcracks and individual cell level defects. In contrast, RPA based overview images of large sections of farms, with up to 1,200 modules contained in a single PL image, as demonstrated here, allow the detection of coarse cell, module, and system-level defects. Quantitative analysis enables accurate assessment of voltage variations within and between modules. The work presented in this paper is a significant step towards commercially viable, fast and effective daylight photoluminescence imaging becoming a routine part of large-scale PV plant inspection.

Acknowledgment

The authors express their sincere gratitude to the management of Wylie's Baths in Coogee for permitting DPL image acquisition, to Wirtgen Invest, owner of the Glenrowan West solar farm for their support, in particular their permission to perform experiments on their premises and Gentari / Wirsol Australia staff, particularly Purnaansh Gunaicha, Matthew Smith and Roshan Dharmasena, for outstanding administrative and technical support during the field work. This work was supported by the Australian Government through the Australian Renewable Energy Agency [ARENA; Project 2022/TRAC013]. The views expressed herein are not necessarily the views of the Australian Government, and the Australian Government does not accept responsibility for any information or advice contained herein.

Conflict of interest

The authors declare that they have no known competing financial interests or personal relationships that could have appeared to influence the work reported in this paper.